Journal of the Korean Ceramic Society
Vol. 40, No. 3, pp. 213~218, 2003.

Band Gap Energy of $SrTiO_3$ Thin Film Prepared by the Liquid Phase Deposition Method

Yanfeng Gao, Yoshitake Masuda, and Kunihito Koumoto†

Department of Applied Chemistry, Graduate School of Engineering, Nagoya University, Nagoya 464-8603, Japan

(Received October 19, 2002; Accepted October 20, 2002)

ABSTRACT

Band gap energies of $SrTiO_3$(STO) thin film on glass substrates were studied in terms of annealing temperature. The STO thin film was fabricated by our newly developed method based on the combination of the Self-Assembled Monolayer(SAM) technique and the Liquid Phase Deposition(LPD) method. The as-deposited film demonstrated a direct band gap energy of about 3.65 eV, which further increased to 3.73 eV and 3.78 eV by annealing at 400°C and 500°C, respectively. The band gap energy saturated at about 3.70 eV for the crystallized film which was obtained by annealing at 600-700°C. The relatively large band gap energies of our crystallized films were due to the presence of minor amorphous phase, grain boundaries and oxygen vacancies generated by annealing in air.

Key words* : *Band gap energy, Strontium titanate, Liquid phase deposition, Crystallinity, Morphology

1. Introduction

Strontium titanate ($SrTiO_3$; STO) in the perovskite structure exhibits high charge storage capacity, good insulating properties and excellent optical transparency in the visible region.[1-3] Thus it is a potential material for a wide range of electronic and optical applications, such as dielectric thin film capacitors in microwave monolithic integrated circuits,[4,5] dynamic random access memory[1,2] and insulating layers for limiting current in thin film electroluminescent displays.[3]

Various growth techniques have been applied to synthesize $SrTiO_3$ thin films. These techniques fall into at least two categories: vacuum-based methods such as Chemical Vapor Deposition(CVD),[6] sputtering,[5] Metalorganic Chemical Vapor Deposition(MOCVD),[7] Atomic Layer Deposition (ALD),[8] and chemical solution methods including sol-gel[9] and hydrothermal synthesis.[10] Vacuum-based techniques are expensive, limited to batch processing, and usually require high-vapor-pressure chemicals or high-purity targets as starting materials. Wet chemical methods mentioned above can overcome some of the demerits of vacuum-based methods by using a homogenous solution, but there are still processing issues, such as control of film thickness at the nanometer scale, professional equipment and complex processes. Direct deposition of $BaTiO_3$ thin film on a silicon substrate by the Liquid Phase Deposition(LPD) method has been reported by Lee *et al.*;[11] the film was grown using an aqueous solution of barium fluorotitanate which was obtained from a mixture of hexafluorotitanic acid and barium nitrate. The Metal-Oxide-Semiconductor(MOS) device using the as-deposited thin film as a gate oxide demonstrated good characteristics of current-voltage and capacitance-voltage. However, the chemical composition of the film was nonstoichiometric,[11] typically Ba/Ti/O=1/10.9/16.5, which might have major effects on the dielectric properties of the annealed film. For example, a large shift of flat band voltage is generated by nonstoichiometry-derived oxygen vacancies, which act as electron donors and high leakage paths.[12]

We developed a novel chemical solution method and successfully deposited STO precursor solid thin films on both the UV-modified Self-Assembled Monolayers(SAMs)[12] and silicon substrates[13] by the LPD method. The SAMs are ultrathin (1.5-3.0 nm) ordered arrays of close-packed long-chain hydrocarbon molecules comprised of base and tail groups at the opposite end of a hydrocarbon chain. UV-irradiation can change the functional group of the SAMs by the photocleavage reaction, altering the hydrophobic property of the surface to hydrophilic property. Growth of the STO precursor solid thin film was well promoted by using the UV-modified SAM surface.

This simple method enables us to deposit the STO precursor solid thin films directly in a $Sr(NO_3)_2$-$(NH_4)_2TiF_6$-H_3BO_3 aqueous solution at an ambient temperature; the film was formed by attachment of homogeneous nuclei generated in the aqueous solution and grew by the Ostwald ripening mechanism. The fabrication of thin films at low temperatures using an aqueous solution shows significant potential to overcome many of the shortcomings of traditional techniques for thin film growth. For example, it is possible to deposit thin films on different substrates such as plastic, silicon, glass, and so on. Hence, it is possible to control the film

†Corresponding author : Kunihito Koumoto
E-mail : g44233a@nucc.cc.nagoya-u.ac.jp
Tel : +81-52-789-3327 Fax : +81-52-789-3201

topography by selecting different substrates, SAMs and/or deposition conditions.

The as-deposited thin film demonstrated stoichiometric composition of Sr/Ti and contained fluorine as a main impurity which was eliminated by annealing at 500°C for 2 h in air. Current-voltage and capacitance-voltage characteristics of MOS devices by using the as-deposited thin film and those annealed as the gate films revealed that the STO thin film fabricated by combining the SAM technique with the LPD method through a one-step process is promising for its application to dielectric films.

Regarding the properties of STO thin films, previous studies[1-5,12] focused mainly on the structure, composition and dielectric properties of the thin films. Only several reports involved characterization of optical properties such as band gap energies.[3,9] Kamalasanan *et al.* reported that sol-gel-derived STO thin film had a band gap energy of 3.43 eV, but no detailed structure information was given.[3] Bao *et al.* prepared STO thin films by the sol-gel method and studied the relationship between band gap energy and crystallinity of STO thin films.[9] They proposed that crystallinity had a large effect on the band gap energy. Poorly crystallized STO thin films demonstrated much larger band gap energies than single crystals, while highly crystallized ones had almost the same band gap energy as single crystals.[9] In addition, they found that the band gap energy was film thickness-dependent and gave a critical thickness of 200 nm. Above 200 nm, the film had a band gap energy close to those of crystals or bulk materials, but below 200 nm, the value shifted largely.[9] However, the effect of the morphology of the thin film on the band gap energy is still unclear, and no report has been published on the band gap energy of amorphous STO thin film. In this paper, we studied changes of the band gap energy of LPD-derived STO thin films in terms of crystallinity and morphology along with the band gap energy of amorphous STO precursor thin film.

2. Experimental

Cleaned barium boronsilicate glasses (1×1 cm; Corning 1737 glass) were exposed to UV irradiation (184.9 nm, 5 W×4 Hg lamps) for 2 h, then immersed in a 1% (vol.) Octadecyltrichlorosilane (OTS)-containing toluene solution for 5 min. under N_2 to prepare SAMs. After drying under nitrogen, the substrates were baked at 120°C for 5 min. in air to improve the adhesion of SAMs. They were then UV-irradiated again for 2 h, which modified the carbon hydrogen chain-terminated OTS-SAMs to silanol groups, changing the hydrophobic surface into a hydrophilic surface. The deposition solution was composed of fresh aqueous solutions of $(NH_4)_2TiF_6$, $Sr(NO_3)_2$, and H_3BO_3 with the molar ratio of 1 : 1 : 3. Deposition of a solid phase was conducted by floating the substrate on the surface of the mentioned solution at 60°C for 1−12 h. After the deposition, the substrate was rinsed with deionized water (>18 MΩcm) before being dried in vacuum at 30°C for 12 h.

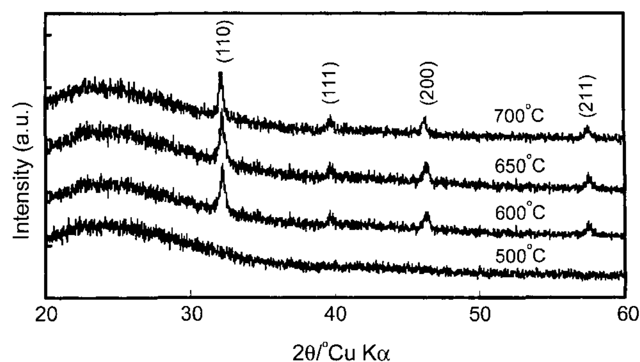

Fig. 1. XRD profiles of the thin films annealed at different temperatures.

Phase composition was measured by X-Ray Diffraction (XRD; RAD-C, Rigaku, Cu Kα, 40 kV, 30 mA). Morphology was characterized by an atomic force microscope (AFM; SPI3800N, Seiko Instruments Inc.) operated under ambient temperature with a scanning frequency of 1−2 kHz. The thickness of the film was measured by a laser ellipsometer (PZ2000, Philips) with an incidence angle of 70° and wavelength of 632.8 nm. Optical transmission spectra were measured by a V-570 spectrophotometer (JASCO, scanning rate: 100 nm · min^{-1}) at room temperature in the wavelength range of 200−1000 nm. Chemical composition was analyzed by an X-ray Photoelectron Spectroscope(XPS; ESCALAB 210, VG Scientific Ltd.; Al Kα, 15 kV, 18 mA).

3. Results and Discussion

Fig. 1 shows the XRD profiles of the as-deposited STO thin film along with those annealed at different temperatures. The as-deposited STO thin film was amorphous and crystallized into perovskite STO after annealing at 600°C for 2 h in air. Increasing temperature resulted in an increase in the crystallinity. The crystal lattice constant calculated using XRD data is 3.865 Å, which is a little smaller than the reported value for STO single crystal (3.905 Å). The crystallization temperature of the STO film in the present study is 100°C higher than that deposited on a heptadecafluoro-1,1,2,2,-tetrahydrodecyltrichlorosilane (HFDTS)-derived silanol surface with p-type silicon as a substrate. We found that the grain size (20−30 nm) of the present film is much smaller than 200 nm of the film deposited on an HFDTS-derived silanol surface with p-type silicon as a substrate. The film thicknesses are both about 200 nm. Hence, we inferred that the changes of grain size or the substrate account for such a difference of crystallization temperature.

Fig. 2 shows the AFM images of the as-deposited thin film deposited on glass substrates. The as-deposited thin film was composed of closely-packed grains of 20−30 nm in diameter. After being heated at 500°C, the film became denser, but no obvious increase in grain size was observed. The sample seems to have been sintered at 700°C. Note no obvious cracks were observed during annealing.

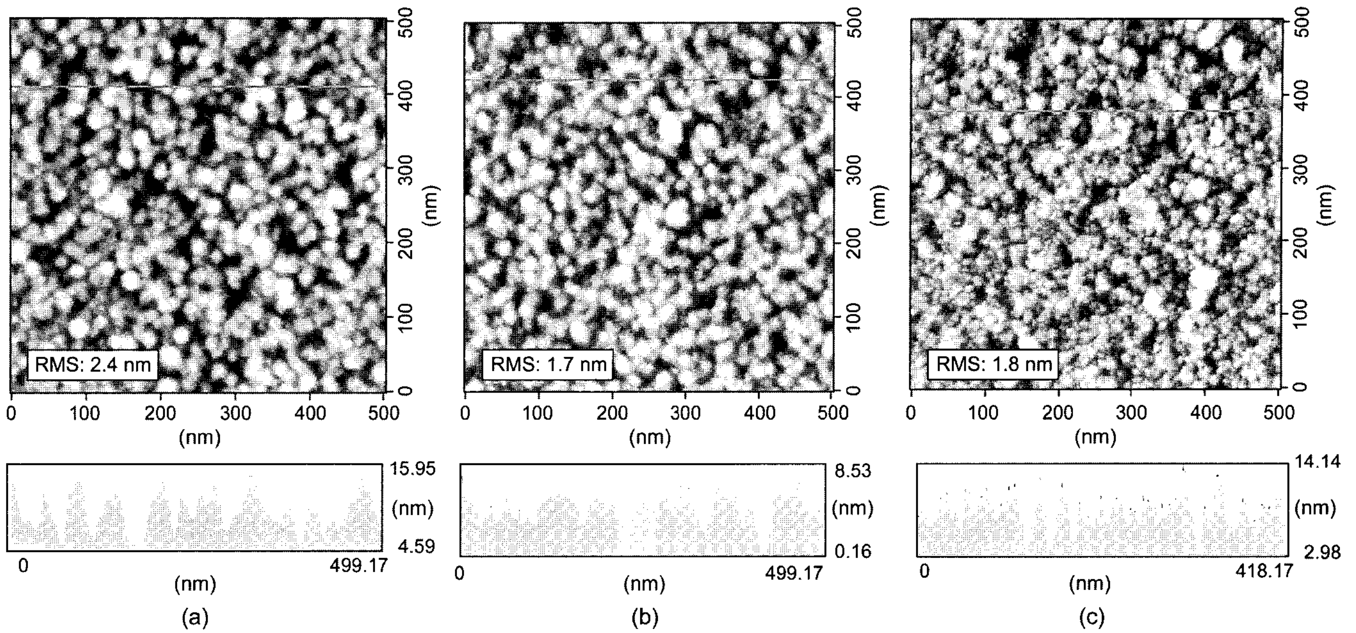

Fig. 2. AFM images of the as-deposited STO precursor solid thin film (a), and those annealed at 500°C (b) and 700°C (c); roughness profiles of the lines shown in the corresponding AFM image; measured areas are all 500×500 nm^2.

The statistical roughness, Root Mean Square(RMS) for the whole measured area (about 500×500 nm^2) was 1.7 – 2.4 nm, indicating the formation of a smooth surface. Both the average grain size and RMS were much smaller than those of the thin film deposited on a silanol surface of the UV-modified HFDTS-SAM, where we obtained an average grain size of 200 nm and an RMS of 10.6 – 12.9 nm for a scan area of about 4×4 μm^2. Although the mechanism accounting for this difference is not well understood, it seems to be related to different nuclei density on the different surfaces. Compared to the OTS-derived silanol surface, the HFDTS-derived silanol surface appears more conductive to the nucleation and growth of a STO precursor solid in three dimensions forming a high density of isolated islands. In any case, the decrease in grain size should help improve the optical properties by increasing the density of the film.

The optical transmission spectra shown in Fig. 3 demonstrated that the film was highly transparent (transmittance ≥82%) in the visible region for both the as-deposited thin film and those annealed at different temperatures. The high transmittance indicates a fairly smooth surface and relatively good homogeneity of the film, which are consistent with the results of AFM observation.

For the high-energy absorption region, the relation between transmittance (T) and absorption coefficient (α) can be expressed as

$$\alpha = -\ln(T)/d \quad (1)$$

where d is the film thickness, neglecting the reflection coefficient, which is negligible and insignificant near the absorption edge.[14]

The relation of absorption coefficient and incident photon energy $h\nu$ can be written as

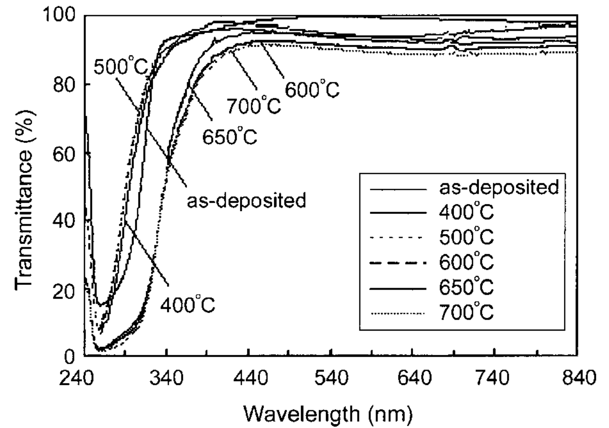

Fig. 3. Optical transmittance spectra of the as-deposited STO precursor solid thin film and those annealed at high temperatures.

$$(\alpha h\nu) = A_1(h\nu - E_g^{\,1})^{1/2} \quad (2)$$

$$\text{and } (\alpha h\nu) = A_2(h\nu - E_g^{\,2})^2 \quad (3)$$

for allowed direct transition and indirect transition, respectively, where A_1 and A_2 are constants, and $E_g^{\,1}$ and $E_g^{\,2}$ are the direct and indirect band gap energies related to direct transition and indirect transition, respectively.[15]

A direct transition occurs when the valence band maximum and the conduction band minimum are at the same point in the Brillouin zone, and an indirect one occurs when the minimum and the maximum are at different places. For a direct transition, a photon with energy $h\nu$ can be absorbed

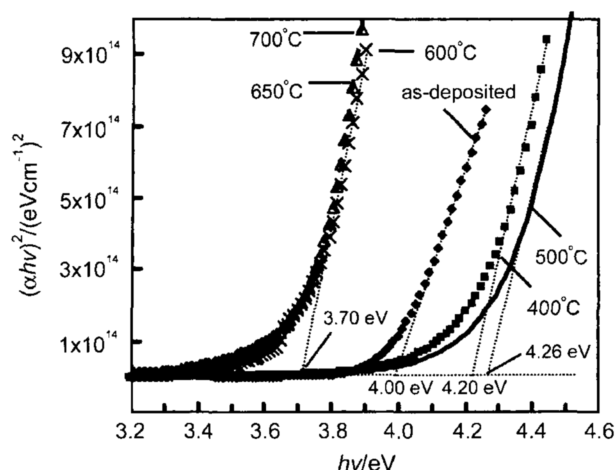

Fig. 4. Direct transition band gap energies of the as-deposited STO precursor solid film and those annealed at different temperatures.

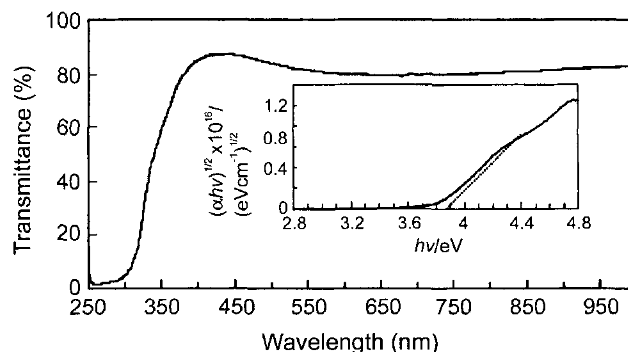

Fig. 5. Optical transmittance spectrum of the $SrTiO_3$ thin film annealed at 700°C in oxygen atmosphere for 2 h; the inset shows its allowed direct band gap energy.

by promoting a valence band electron to the conduction band, creating an electron-hole pair. This process involves a two-body collision (electron and photon) accompanied by strong light absorption, whereas for an indirect transition between two bands with different wavevectors, both the kinetic energy and the potential energy of an electron must be changed, which requires the assistance of a phonon. Hence, this process involves a three-body collision (electron, photon and phonon) and relatively weak light absorption.

The usual method of determining band gap energy is to plot a graph between $(\alpha h\upsilon)^n$ (n=2 or 1/2 for direct allowed transition and indirect transition) and photon energy $h\upsilon$, and to compare which value of n gives the best linear relation in the band edge region. We plotted $(\alpha h\upsilon)^n$ against $h\upsilon$ for the as-deposited thin film and those annealed at different temperatures, and found the best fit was obtained for n= 2, indicating a direct allowed transition as shown in Fig. 4. Moreover, a fast increase of absorption around the absorption edge is observed in Fig. 3, which is characteristic of the direct transition.

Annealing at high temperatures, such as 600°C, 650°C and 700°C, the band gap energies were saturated to about 3.70 eV, comparable to that for a sol-gel-derived thin film with the thickness of 150 nm.[9] However, it is higher than that for the single crystal (3.37 eV−3.41 eV),[16,17] except that proposed in the reference 18 (3.75 eV). Such a difference might be due to three possible reasons: (1) poor crystallinity. As we discussed before, in the defect-free crystalline $SrTiO_3$, the adsorption edge should be terminated at the energy gap. However, for our annealed samples (see Fig. 3) including that annealed at 700°C for 2 h in oxygen atmosphere (see Fig. 5), absorption tails could still be observed, suggesting that absorption occurred below the gap. This indicated the presence of minor amorphous phases such as $SrCO_3$. Tcheliebou and co-workers obtained a high E_g value of 3.96 eV for $Ba_{0.5}Sr_{0.5}TiO_3$ thin film and suggested it accounted for the existence of an amorphous phase;[19] (2) the existence of grain boundaries in the polycrystalline thin film.[9] A difference of the atomic structure between the grain boundary and the grain causes the formation of an additional electric field and increases band gap energy; and (3) the presence of oxygen vacancies, which we will discuss below.

We have found a large flat-band shift along the voltage axis in the capacitance-voltage characteristics of an MOS device with an air annealed STO thin film as a gate oxide layer, indicating the formation of positively charged defects. No residual fluorine was detected by XPS analysis, therefore such defects were attributed to oxygen deficiency generated during annealing according to the following defect equation expressed by the Kröger-Vink notation:[12]

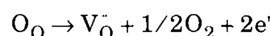

$$O_O \rightarrow V_O^{\cdot\cdot} + 1/2O_2 + 2e'$$

A similar phenomenon has been experimentally observed. Gandy[20] reported that the vacuum heating of pure, stoichiometric $SrTiO_3$ crystals has a reducing effect on them causing a loss of oxygen from their perovskite lattice accompanied by a strong attendant absorption, which could be removed by heating the crystals in oxygen again.

For such a film, optical excitation enables electrons and holes to be created in the conduction band and valence band, respectively. These carriers can then be trapped at the donor (marked as D^+) and acceptor sites (A^-) to produce neutral D^0 and A^0 centers. This process is known as a donor-acceptor pair transition (DAP transition), and can be represented by the reaction[15]

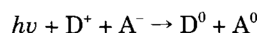

$$h\upsilon + D^+ + A^- \rightarrow D^0 + A^0$$

In this case, the band gap energy can be represented as[15]

$$E_g = h\upsilon + E_A + E_D - e^2/(\varepsilon R),$$

where E_g is the band gap energy, $e^2/(\varepsilon R)$ is Coulomb energy, and E_D and E_A are the donor and acceptor binding energies, respectively. It is obvious that additional donors and/or acceptors can increase the band gap energy of an oxide.

When the sample were heated at 700°C in oxygen atmosphere for 2 h, as shown in Fig. 5, no obvious change in the

absorption spectrum was observed and the band gap energy of 3.81 eV assuming an allowed direct transition was obtained, which was comparable to that for the samples heated in air. The compensation of oxygen defects by increasing partial pressure of oxygen during annealing was not confirmed under the present conditions. In Gandy's[20] experiment by heating pure $SrTiO_3$ in vacuum, the oxygen defects began to be induced at about 850°C, suggesting that the lowest temperature for sufficient oxygen diffusion was around 850°C. The generation of oxygen vacancies in our films was closely related to the decomposition of fluorine, especially accompanied by the crystallization, since flatband shifts were not observed for the as-deposited film. However, it appears necessary to anneal at a higher temperature than 700°C in oxygen to remove such defects. This temperature is too high for the present substrate material, which prevented us from giving an experimental confirmation.

Additionally, the grain size remained at nanometer order even after heating above 600°C from the results of both XRD and AFM, indicating that no quantum-size effect on the shift of band gap energy was achieved.

Band gap energies of the films in the amorphous state were also discussed. The as-deposited STO precursor solid film (203 nm) gave a band gap energy of 4.0 eV when calculated by using equation (2) (see Fig. 4). After annealing at 400°C or 500°C, the band gap energies increased to 4.26 eV and 4.20 eV, respectively (see Fig. 4). All of them were much larger than those of the single crystals (3.37 eV–3.41 eV,[16,17] 3.75 eV).[18] Our as-deposited thin film and those annealed at 400°C or 500°C were amorphous containing fluorine as a major impurity, which may be responsible for such a difference. After annealing at 500°C, the binding energies for $Sr_{3d5/2}$, $Ti_{2p3/2}$ and O_{1s} were 133.5 eV, 459.0 eV and 530.5 eV, comparable to those obtained for the film on the HFDTS-SAMs.[12,13] However, residual fluorine was also detected by XPS (see Fig. 6), indicating that the large band gap energy might be not because of defects such as oxygen vacancies.

In fact, in a defect-free crystalline semiconductor, the absorption spectrum terminates abruptly at the wavelength corresponding to the energy gap. No absorption is observed below that wavelength. Hence, one can define the absorption edge of a crystalline semiconductor experimentally. In contrast, in an amorphous semiconductor, a tail in the absorption spectrum encroaches into the gap region. This tail state is usually localized by the site disorder, and a critical energy, called the mobility edge, separates the localized state from the extended state. The existence of a tail state makes it difficult to define the absorption edge experimentally. As a consequence, various empirical measures have been proposed. The Tauc gap[21] is often used to characterize the optical properties of amorphous materials. The Tauc gap determines the absorption of light at high energies (above the gap energy) or short waves. This can be represented by equation (3). Therefore, this may lead to large errors when calculating the band gap energy of an amorphous thin film.

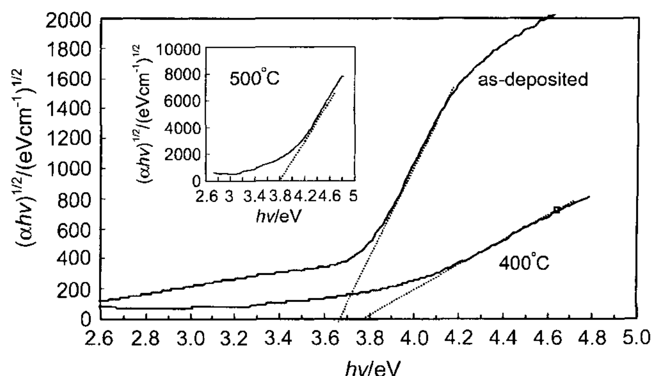

Fig. 7. Tauc gaps of the as-deposited thin film and those annealed at 400°C and 500°C (inset).

We also calculated the so-called Tauc gaps for our amorphous films. As shown in Fig. 7, 3.65 eV, 3.73 eV and 3.78 eV were obtained for the as-deposited thin film, which was annealed at 400°C and 500°C, respectively. These values are in agreement with the data obtained for the crystallized thin film.

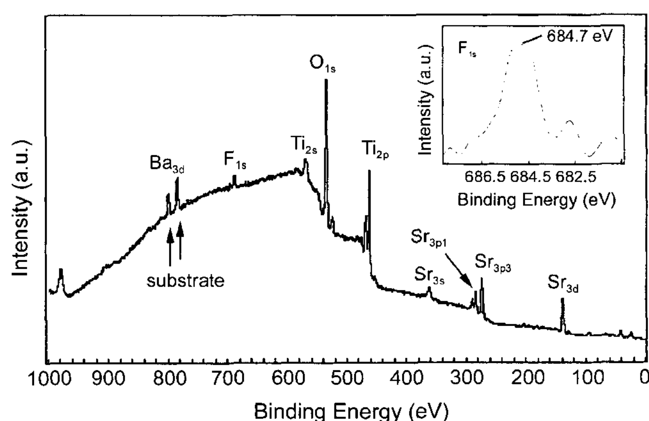

Fig. 6. Wide-range XPS spectrum of the $SrTiO_3$ thin film annealed at 500°C in air; the inset shows the F_{1s} range.

4. Conclusions

In summary, we investigated the band gap energies of $SrTiO_3$ thin films which were prepared by our newly developed low temperature process. The as-deposited film and those annealed at 400°C and 500°C demonstrated band energies in the range 3.65–3.78 eV, which saturated at 3.70 eV for the crystallized film. The band gap energy was higher than that of a single crystal, which was due to the presence of a minor amorphous phase, grain boundaries and oxygen defects formed during annealing in air.

Acknowledgement

One of our authors (Y.-F. G.) is grateful to NGK Insulators Ltd. (Japan) for providing a scholarship.

REFERENCES

1. A. F. Tasch, Jr. and L. H. Parker, "Memory Cell and Technology Issues for 64- and 256-Mbit One-transistor Cell MOSD DRAMs," *Proc. IEEE*, **77** 374-88 (1989).
2. P. C. Joshi and S. B. Krupanidhi, "Structural and Electrical Characteristics of $SrTiO_3$ Thin Films for Dynamic Random Access Memory Applications," *J. Appl. Phys.*, **73** 7627-34 (1993).
3. M. N. Kamalasanan, N. D. Kumar, and S. Chandra, "Structural, Optical, and Dielectric Properties of Sol-gel Derived $SrTiO_3$ Thin Films," *J. Appl. Phys.*, **74** 679-86 (1993).
4. T. Kunihisa, S. Yamamoto, M. Nishijima, T. Yokohama, M. Nishitsuji, K. Nishii, and O. Ishikawa, "Low Power Dissipation Single-supply MMIC Power Amplifier for 5.8 GHz Electronic Toll Collection System," *IEICE Trans. Electron.*, **E82-C** 1921-27 (1999).
5. K. Morito, H. Wakabayashi, T. Suzuki, and M. Fujimoto, "Fabrication Technology of High-dielectric $SrTiO_3$ Thin Film Capacitors for Microwave Circuits," *J. Ceram. Soc. Jpn.*, **110** 408-15 (2002).
6. H. Funakubo, Y. Takeshima, D. Nagano, A. Saiki, K. Shinozaki, and N. Mizutani, "Deposition Conditions of $SrTiO_3$ Thin Films on Various Substrates by CVD and their Dielectric Properties," *Thin Solid Films*, **334** 71-6 (1998).
7. K. Fröhlich, D. Machajdík, A. Rosová, F. Weiss, B. Bochu, J. P. Senateur, and I. Vávra, "Growth of $SrTiO_3$ Thin Epitaxial Films by Aerosol MOCVD," *Thin Solid Films*, **260** 187-91 (1995).
8. M. Vehkamäki, T. Hänninen, M. Ritala, M. Leskelä, T. Sajavaara, and J. Keinonen, "Atomic Layer Deposition of $SrTiO_3$ Thin Films from a Novel Strontium Precursor-Strontium-bis(tri-isopropyl cyclopentadienyl)," *Chem. Vapor Deposition*, **7** 75-80 (2001).
9. D. Bao, X. Yao, N. Wakiya, K. Shinozaki, and N. Mizutani, "Band-gap Energies of Sol-gel-derived $SrTiO_3$ Thin Films," *Appl. Phys. Lett.*, **79** 3767-69 (2001).
10. M. Yoshimura, W. L. Suchanek, T. Watanabe, and B. Sakurai, "*In Situ* Fabrication of $SrTiO_3$-$BaTiO_3$ Layered Thin Films by Hydrothermal-electrochemical Technique," *J. Euro. Ceram. Soc.*, **19** 1353-59 (1999).
11. M. K. Lee, K. W. Tung, C. C. Cheng, H. C. Liao, and C. M. Shih, "Deposition of Barium Titanate Films on Silicon by Barium Fluorotitanate Powder," *J. Phys. Chem. B*, **106** 4963-66 (2002).
12. Y. Gao, Y. Masuda, T. Yonezawa, and K. Koumoto, "Site-selective Deposition and Micropatterning of $SrTiO_3$ Thin Film on Self-assembled Monolayers by the Liquid Phase Deposition Method," *Chem. Mater.*, **14** [12] 5006-14 (2002).
13. Y. Gao, Y. Masuda, T. Yonezawa, and K. Koumoto, "Preparation of $SrTiO_3$ Thin Film by the Liquid Phase Deposition Method," *Mater. Sci. and Eng. B.*, in press.
14. L.-J. Meng and M. P. Dos Santos, "Investigation of Titanium Oxide Films Deposited by D. C. Reactive Magnetron Sputtering in Different Sputtering Pressures," *Thin Solid Films*, **226** 22-9 (1993).
15. P. Y. Yu and M. Cardona, *Fundamentals of Semiconductors*, p.343 (Springer, Berlin **1996**).
16. G. A. Barbosa, R. S. Katiyar, and P. S. Porto, "Optical Properties of $SrTiO_3$ at High Temperatures," *J. Opt. Soc. Am.*, **68** 610-14 (1978).
17. S. Zollner, A. A. Demkov, R. Liu, P. L. Fejes, R. B. Gregory, P. Alluri, J. A. Curless, Z. Yu, J. Ramdani, R. Droopad, T. E. Tiwald, J. N. Hilfiker, and J. A. Woollam, "Optical Properties of Bulk and Thin-film $SrTiO_3$ on Si and Pt," *J. Vac. Sci. Technol. B*, **18** 2242-54 (2000).
18. K. V. Benthem, C. Elsässer, and R. H. French, "Bulk Electronic Structure of $SrTiO_3$: Experiment and Theory," *J. Appl. Phys.*, **90** 6156-64 (2001).
19. F. Tcheliebou, H. S. Ryu, C. K. Hong, W. S. Park, and S. Baik, "On the Microstructure and Optical Properties of $Ba_{0.5}Sr_{0.5}TiO_3$ Films," *Thin Solid Films*, **305** 30-4 (1997).
20. H. W. Gandy, "Optical Transmission of Heat-treated Strontium Titanate," *Phys. Rev.*, **113** 795-800 (1959).
21. J. C. Tauc, *Amorphous and Liquid Semiconductor,* p.159 (Plenum, New York, **1974**).